DOI: 10.1002/geot.202000046

Clemens Proksch-Weilguni, Hannes Wolfger, Johann Kollegger

Optimized reinforcement in longitudinal joints of segmental tunnel linings

When building tunnels using segmental lining, the segmental lining takes over the supporting role of the excavated soil. With the workspace in tunnel construction being very constricted the circular, segmental linings are divided into small segments called tubbings which are assembled by a tunnel boring machine. This kind of construction results in numerous longitudinal and circumferential joints. The loading situation for the longitudinal joints is typically dominated by the compressive normal forces combined with relatively small bending moments. The thickness of the tubbings usually depends on the longitudinal joints of the individual segments. The cross-sectional area of the tubbings has to be reduced at the joints in order to avoid spalling of the concrete leading to higher compression in the joints themselves. The Institute of Structural Engineering of TU Wien developed a new reinforcement design for tubbings with strengthened longitudinal joints. With a patent application pending, the newly designed joints were manufactured and tested demonstrating that the TU Wien proposal significantly increases the load-bearing capacity of the tubbings in comparison to conventional tubbing solutions. The very satisfying results, obtained from the large-scale tests of the newly developed joint design, show great potential for the construction of tunnels with thinner tubbings in the near future.

Keywords Precast tunnel segments; tubbing; joint reinforcement; innovative design

Optimiertes Bewehrungskonzept für Tübbing-Längsfugen im Segmenttunnelbau

Bei der Errichtung von Tunneln mit Fertigteilsegmenten übernimmt die Tunnelschale die Tragwirkung des ausgebrochenen Gebirgsmaterials. Da die Platzverhältnisse im Tunnelbau stark beschränkt sind, ist die Tunnelschale in einzelne Segmente unterteilt. Die Begrenzungsflächen zwischen den Tübbingen werden in Längs- und Ringfugen unterteilt. In den Tübbing-Längsfugen sind typischerweise hohe Drucknormalkräfte in Kombination mit relativ kleinen Biegemomenten vorherrschend. Für die Dicke der Tübbinge ist häufig die Bemessung der Tübbing-Längsfugen maßgebend. Dies resultiert aus dem Umstand, dass die Regelquerschnittsfläche der Tübbinge im Bereich der Längsfugen reduziert werden muss, um ein Abplatzen der Betonkanten zu verhindern. Die dadurch entstehenden hohen Druckspannungen im Bereich der Tübbinglängsfugen sind ein wesentlicher Faktor bei der Bemessung der Tübbinge. Das Institut für Tragkonstruktionen der TU Wien hat ein neues Bewehrungskonzept für Tübbinge entwickelt, dass zu einer Verbesserung der Tragfähigkeit der Tübbing-Längsfuge führt. Basierend auf einer Patentanmeldung der TU Wien wurde das optimierte Bewehrungskonzept in einer Versuchsserie getestet und gezeigt, dass das optimierte Bewehrungskonzept die Tragfähigkeit der Tübbinge signifikant steigert. Die Großversuche lieferten sehr zufriedenstellende Ergebnisse und lassen auf das große Potenzial für den Bau von dünneren und tragfähigeren Tunnelschalen schließen.

Stichworte Fertigteilsegmente; Tübbing; Bewehrung Tübbing-Längsfuge; innovatives Design

1 Introduction

The fast technical evolution of tunnel boring machines (TBM) in the past decades contributed to the high popularity of the continuous tunnelling method. Due to the adaptivity of the TBM setup, it became possible to drive tunnels through all kinds of difficult soil and water conditions in a safe, quick and economic way. In the case of a very long tunnel the dimension of the tunnel structure, which influences the excavated cross section, has a huge impact on the total costs of the infrastructure project. The clearance needed for traffic is a factor that simply cannot be reduced, leaving only the thickness of the tunnel lining, to be variable. The thickness of the tubbings then again depends on the load-bearing capacity of the longitudinal joints (Figure 1) of the individual construction segments. There the cross-sectional area of the tubbings has to be reduced in order to avoid spalling of the concrete leading to higher compression in the joints themselves ($\sigma_{c0} > \sigma_{c1}$ as can be seen in Figure 1).

This paper discusses the state of the art of the ultimate limit state (ULS) design according to the European standards [1, 2] and presents a new optimized reinforcement design for tubbings with strengthened longitudinal joints. Although there are no analytical models available, a couple of empirical models [3–6] that describe this specific problem of partially loaded areas in longitudinal joints of tubbings can be found. These models are based on experiments leading to limitations when it comes to applying the models to different configurations or systems. Based on this gathered knowledge the newly developed joint design, invented and patented in 2019 by the Institute for Structural Engineering of TU Wien [7, 8], as well as first test results and a suggestion on how to adapt the existing empirical models to calculations of

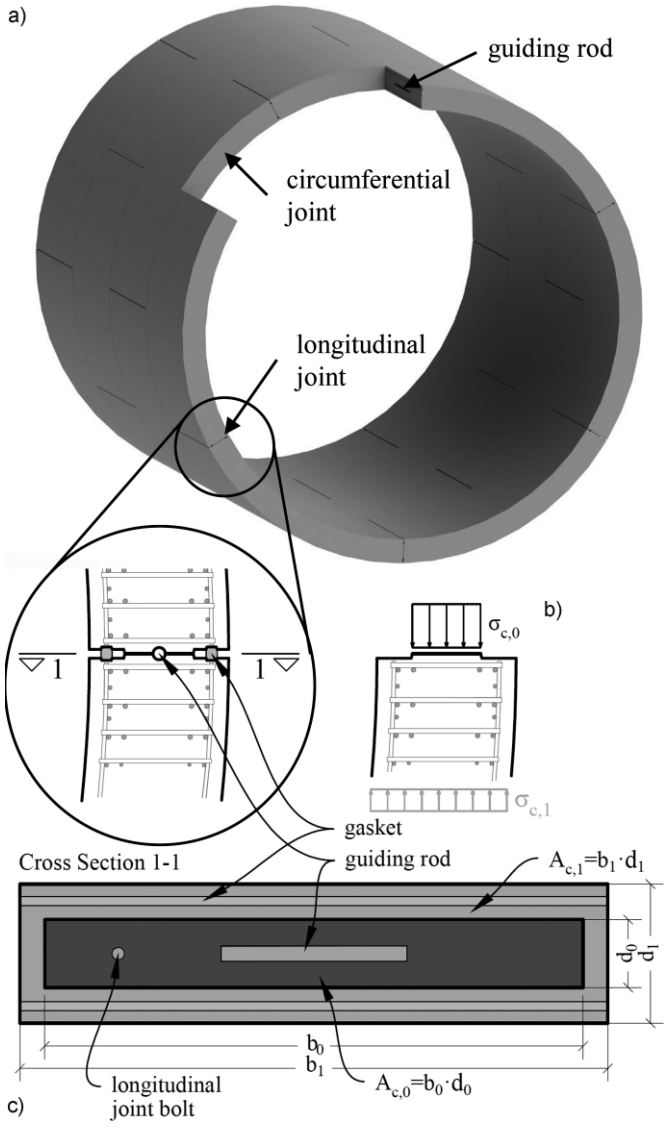

Fig. 1 a) Segmental tunnel lining structure; b) longitudinal joint detail (left), longitudinal joint stress distribution (right); c) longitudinal joint cross section

the load-bearing capacity of the longitudinal joints of tubbings are presented.

2 State of the art

For tunnels located in large depths with predominant loads caused by soil pressure, the internal forces are typically dominated by compressive normal forces combined with relatively small bending moments. In these cases, the thickness of the tunnel tubbings according to state-of-the-art design is dependent upon the cross section of the longitudinal joints. The area of the tubbings has to be reduced in the joints in order to avoid spalling of the concrete due to relative rotations of the segments and enable a placement of the necessary watertight gasket. In addition, the reduced cross section in the longitudinal joints must still be able to transfer the compression forces. To meet the mentioned geometric requirements the cross section of the longitudinal joint (A_{c0}) is reduced approx. to half the size of the regular cross section of the tubbing (A_{c1}), leading to a two times higher stress level (see Figure 1). In the past various solutions for this problem had been considered. An overview of these already existing solutions and a walk through the ULS design according to current available design approaches applied to a conventional longitudinal joint are discussed in Section 2.1 and 2.2. In this paper only the centrically loaded longitudinal joint is presented and discussed, because the following experiments were done for a centric load situation without bending moments.

2.1 Existing solutions for increasing the load-bearing capacity in the longitudinal joint

A variety of solutions to increase the load-bearing capacity of longitudinal joints of tubbings have been invented. None of these is state of the art when it comes to designing an economic tunnel. Even though every building or concrete structure is unique, it is often cheaper to oversize details instead of optimizing them. For most projects it is more profitable to optimize the building process or reduce the working hours than optimize a technical detail and minimize the material consumption. In the case of tunnelling the optimization of the tubbings, especially when it comes to their thickness, can save a lot of money, not only because of the material economization but also because of the savings in excavating. Furthermore, if expensive strengthening elements and complex manufacturing steps, which significantly increase the total costs of a tunnel project, can be reduced, an optimization of the joints is highly valued.

2.1.1 Patent application AT 518840 A1

One possibility to increase the load-bearing capacity of the tubbing longitudinal joint is described in the patent application of Porr Bau GmbH [9]. In the solution shown in Figure 2a the cross section of the tubbing is made of reinforced concrete and the area next to the longitudinal joint is strengthened using a material with a significant higher compressive strength, as for example steel or stainless steel. The chosen dimensions of the strengthening bodies must guarantee a distributed load transmission into the regular cross section of the tubbing. Disadvantages comprise of the high costs of the strengthening bodies, a higher probability of corrosion and the negative impact on the load-bearing capacity in case of fire [9].

2.1.2 Patent EP 1 243753 B1

In the joint solution shown in Figure 2b the strengthening bodies are coupling elements out of steel which increase the load-bearing capacity of the longitudinal joints. Each joint comprises of two distinct coupling elements creating a form fitting connection. The coupling elements are anchored with reinforcement bars or anchors to distribute the concentrated compression forces from the joint into the

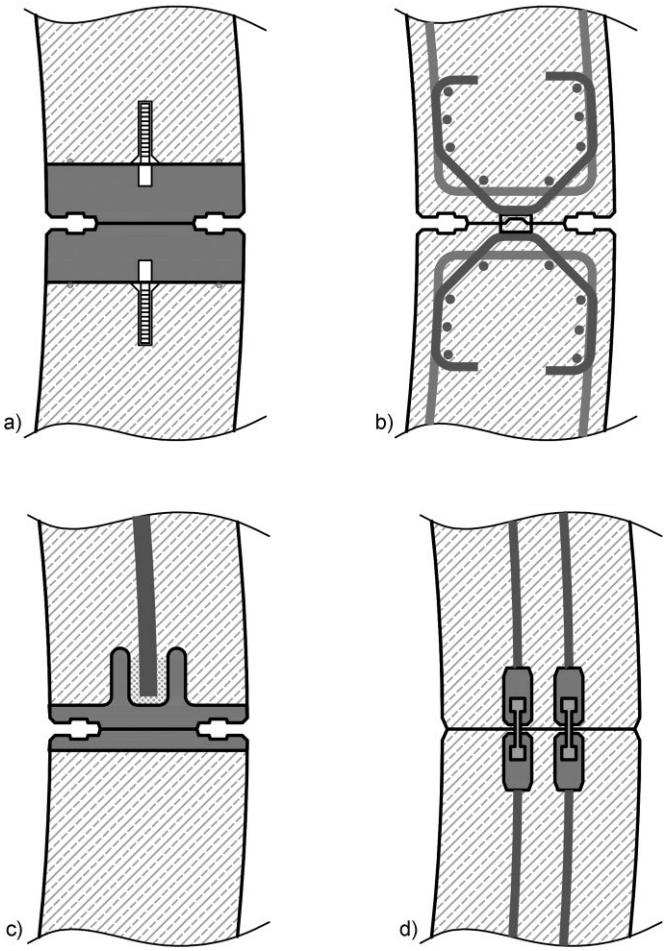

Fig. 2 Schematic drawings of different patent applications: a) Patent application Porr Bau GmbH 2016, strengthening bodies out of steel; b) Patent Dahl 2002, coupling elements anchored by reinforcement stirrups; c) Patent Oger 1977, strengthening bodies out of cast iron and longitudinal steel elements; d) Patent application Hirohide and Susumu 1999, C-shaped steel elements anchored with screwed reinforcement

standard cross section of the tubbing element [10]. Disadvantages include the costs of the coupling elements and the susceptibility to corrosion of the steel coupling elements.

2.1.3 Patent DE 25 22 789 C3

In the joint solution described by Oger [11] and pictured in Figure 2c the load-bearing capacity is increased by strengthening bodies made of cast iron and longitudinal steel elements. The axial compressive force is transferred from the longitudinal steel elements through the cast-iron element into the second tubbing strengthening body. The longitudinal elements are welded to the cast iron elements. The high costs of the cast iron elements and the corrosion problem are the main reasons why this system is not used in practical applications.

2.1.4 Patent application JP 11287093 A

The Japanese patent application shown in Figure 2d does not consider the usual reduction of the cross section in

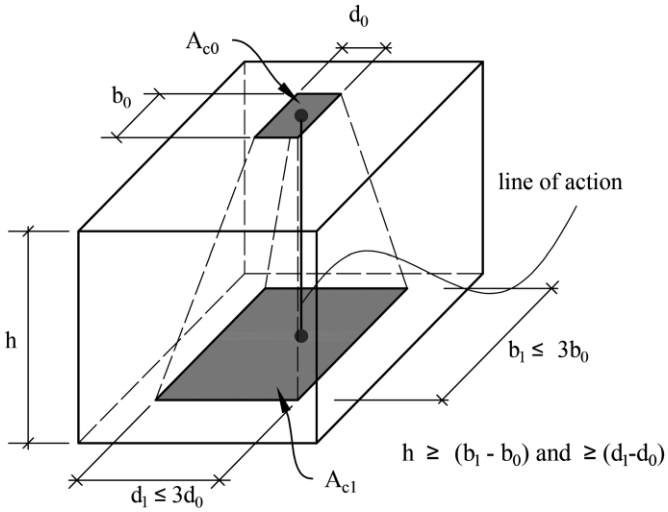

Fig. 3 Design distribution for partially loaded areas according to EC2 [1]

the area of the longitudinal joint. C-shaped steel elements, which are anchored in the tubbing with screwed-in reinforcement bars, are placed at the surface of the longitudinal joint and are connected with engaging counterparts. The patent application explains that there is a gap between the end faces of the C-shaped steel elements disabling a transfer of the axial compression forces in the longitudinal joints. The compression force is just able to be transferred through the engaging counterparts [12].

2.2 Design approaches of the longitudinal joints

In this section the ULS design according to current available design approaches applied to a conventional longitudinal joint are discussed.

2.2.1 Eurocode 2 applied in the guideline of the German Tunnelling Committee

In Europe the most commonly used analysis method for longitudinal joints of tubbings recommended for example by the German guideline (DAUB) [3] and the Austrian guideline (ÖVBB) [4] for designing tubbings is the method according to EC2 [1], Section 6.7 (shown in Eq. 1). This approach applies the effect of a partially loaded area which leads to a multiaxial-stress state to increase the compressive strength of the investigated concrete. According to EC2 [1] the areas A_{c0} and A_{c1} have to be similar in shape (as shown in Figure 3) and there must be sufficient transversal reinforcement installed for the existing transverse tension forces. As can be seen in Eq. 1 there is no explicit consideration of the transversal reinforcement in the approach of EC2 [1].

The special case of longitudinal joints of tubbings is discussed for example in [3, 5] where it is stated that for the specific geometric case of the longitudinal joint and with sufficient transversal reinforcement the strict geometrical requirements can be neglected. Taking this into consider-

ation A_{c1} in Eq. 1 equals the regular cross section of the tubbing shown in Figure 1 ($A_{c1} = b_1 \cdot d_1$). Even though there is no analytical model supporting this assumption, the results of several experiments summarized in [3] validate it. The resistance force ($F_{cal,EC2}$) of a partial loaded area can be calculated according to Eq. 1.

$$F_{cal,EC2} = A_{c0} \cdot f_{cd} \cdot \sqrt{\frac{A_{c1}}{A_{c0}}} \leq 3{,}0 \cdot f_{cd} \cdot A_{c0} \tag{1}$$

with

f_{cd} Design value of concrete compressive strength
A_{c0} Loaded area
A_{c1} Maximum design distribution area with a similar shape to A_{c0}

The theoretical upper limit for $F_{cal,EC2}$ ($3 \cdot f_{cd} \cdot A_{c0}$) will never be reached for a typical tubbing geometry ($b_1 \approx b_0$) because of the plane load distribution requirement ($d_1 < 3\ d_0$) shown in Figure 3. As stated in [13] the practical upper limit is about $\sqrt{3} \cdot f_{cd} \cdot A_{c0} \approx 1.73 \cdot f_{cd} \cdot A_{c0}$.

In the guideline of DAUB [3] there is a recommendation for determining the transversal reinforcement according to Eq. 2 based on the approach of Mörsch [14] supplemented by Grasser und Thielen [15]. It is also stated how to design the reinforcement for eccentric loaded longitudinal joints. Since the experiments in this paper only cover centric loaded longitudinal joints the eccentric case of determining the splitting reinforcement is not discussed furthermore.

$$F_{S,DAUB} = 0.25 \cdot N_{ed} \cdot \left(1 - \frac{d_0}{d_1}\right) \tag{2}$$

with

$F_{S,DAUB}$ Splitting force to be covered by splitting reinforcement
N_{ed} Maximum normal force
d_0 Shown in Figure 3
d_1 Shown in Figure 3

The recommended centre of gravity of the determined splitting reinforcement according to the guideline of DAUB [3] should be at a distance of $0.4 \cdot d$ from the partially loaded surface and is shown in Figure 5. This is the most commonly used approach for the ULS design of a longitudinal joint of a tubbing and has been applied in several already existing projects. The disadvantages are that the confining effects of the transversal reinforcement is just considered through the requirements for the sufficient transversal reinforcement.

2.2.2 Wichers (2013)

In his dissertation Wichers [16] developed a design approach based on the model of Wurm and Daschner [17]. The theory states that the load-bearing capacity of a partially loaded area consists of two mechanisms; the bearing capacity of the unreinforced concrete ($q_{1u,c}$) and the bearing capacity of the transversal reinforcement ($\Delta q_{1u,s}$). The approach distinguishes between a plain and a volumetric load distribution. According to the definition in [16, 17] the geometry of a typical longitudinal joint is categorized as a plain load distribution. The load-bearing capacity ($F_{cal,Wichers}$) can be determined using Eq. 3 where f_{cm} is the mean value of the concrete compressive strength.

$$F_{cal,Wichers} = A_{c0} \cdot f_{cm} \cdot \left(q_{1u,c} + \Delta q_{1u,s}\right) \tag{3}$$

Regarding the concrete capacity share ($q_{1u,c}$), Eq. 4 differentiates between the well-known cubic root approach [18] for plain load distributions and the square root approach [19] for volumetric load distributions.

$$q_{1u,c} = \begin{cases} \sqrt[3]{\dfrac{A_{c1}}{A_{c0}}} & \text{plain load distribution} \\ \sqrt{\dfrac{A_{c1}}{A_{c0}}} & \text{volumetric load distribution} \end{cases} \tag{4}$$

The load-bearing share of the transversal reinforcement ($q_{1u,s}$) is considered by the terms of Eq. 5. The empirical factor R regulates the linear increase of the bearing capacity in dependence of the geometrical reinforcement ratio ρ_{1d} [%]. The geometrical reinforcement ratio ρ_{1d} is limited to 1 % for a plain load distribution. The factor R also depends on the type of load distribution. In the case of plain load distribution according to Wichers [16] for determination of ρ_{1d} [%] b_0 is equal to b_1. For a typical geometry of a longitudinal joint it is suggested to determine ρ_{1d} as shown in Figure 4.

$$\Delta q_{1u,s} = R \cdot \rho_{1d} = \begin{cases} 0{,}15 \cdot \rho_{1d} & \text{plain distribution} \\ 0{,}55 \cdot \rho_{1d} & \text{volumetric distribution} \end{cases} \tag{5}$$

The recommended location of the centre of gravity of the splitting reinforcement should be at a distance of $0.3 \cdot d$ from the partially loaded surface (Figure 5). Wichers [16] suggests to distribute the chosen splitting reinforcement uniformly with a maximum centre to centre distance of $d/8$.

The advantage of this approach is the direct consideration of the transversal reinforcement ratio in the mechanical model of the load-bearing capacity. It has to be stated that the reinforcement ratio is limited to 1 % which is usually always exceeded in a conventional tubbing design. This approach is based on investigations of centric partially loaded members and, as shown by Schmidt-Thrö [6], underestimates the load-bearing capacity of members with an increased A_{c1}/A_{c0} ratio, a situation which is typical for eccentrically loaded longitudinal joints.

2.2.3 Schmidt-Thrö

The third mechanical model which is presented in this paper was developed by Schmidt-Thrö [6] in 2019 as part

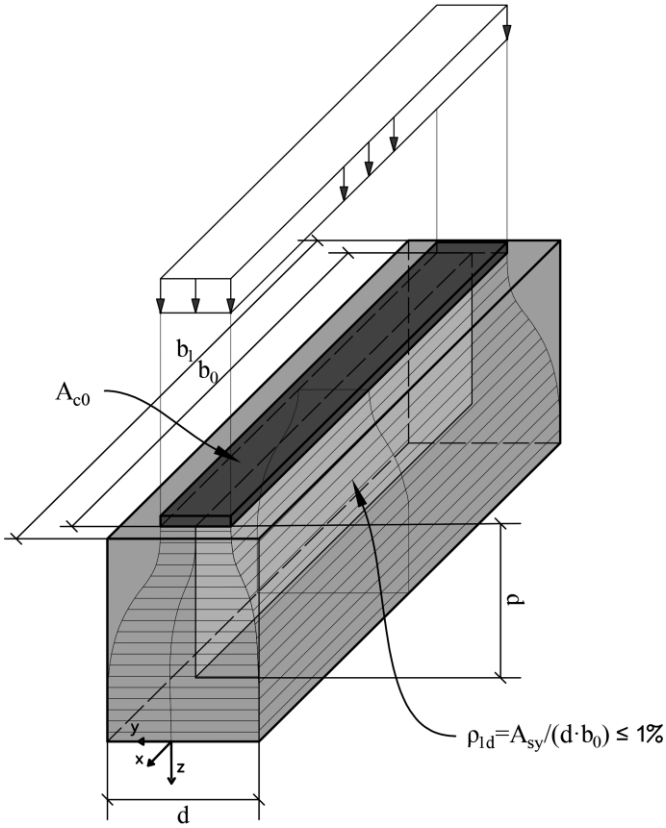

Fig. 4 Design approach Wichers [16]: Load distribution and definition of ρ_{1d} applied to a longitudinal tubbing joint

of his dissertation. After analysing previous experiments further 32 tests were conducted focusing on longitudinal joints with large bending moments leading to eccentricities. One of his two solutions for this specific problem is shown in Eq. 6.

$$F_{\text{cal,Schmidt-Thrö}} = A_{c0} \cdot f_{cm} \cdot \left(0.37 \cdot \frac{A_{c1}}{A_{c0}} + 0.76 \right) \tag{6}$$

For determining the splitting reinforcement (F_s), Schmidt-Thrö recommends the same approach as used in DAUB [3] which can be calculated using Eq. 2. The location of the splitting reinforcement recommended by Schmidt-Thrö [6] differs from the approach in [3] and distinguishes between two areas. In the first area next to the partially loaded surface (first reinforcement layer) 20 to 25 % of the splitting reinforcement F_s have to be placed. The remaining share of 75 to 80 % has to be placed distributed along the distance d with the centre of gravity in a distance of about 0.45 to 0.55 · d from the partially loaded surface.

Schmidt-Thrö focused in his dissertation on the specific geometrical parameters of longitudinal joints. With his experiments being mainly eccentric loaded a higher A_{c1}/A_{c0} ratio is obtained for the theoretical model. This approach was therefore, on the one hand, developed for the design of longitudinal joints of tubbings especially by considering the problem of eccentricities. On the other hand, the impact of the transversal reinforcement is not directly taken into account. Which is at least a disadvantage when it comes to the optimization of a tubbing.

3 Continuous reinforced longitudinal joint

The origin of the idea, the development and the experimental tests carried out with the new design are briefly summarized in this section of the paper. Detailed information of the experimental investigations are presented in Wolfger et al. [20].

In order to increase the load-bearing capacity of the area of the longitudinal joints in tubbings the Institute of Structural Engineering of TU Wien developed an optimization of the reinforcement design. The idea is to place reinforcement in the tubbings, as shown in Figure 6, in such a way that the end sections of the reinforcement bars are located right next to the surface of the longitudinal joints. The resulting compression force in the tubbing segment ring can therefore be transferred by contact stresses in the butt joints of the reinforcement. As shown above using this method the force, which can be carried by the longitudinal joint, can be increased to the level of the load-bearing capacity of the regular tubbing cross section. Therefore, the longitudinal joint reinforcement has to be placed in the area next the longitudinal joint to strengthen the joint. With this approach the ULS design for longitudinal joints in tubbings without

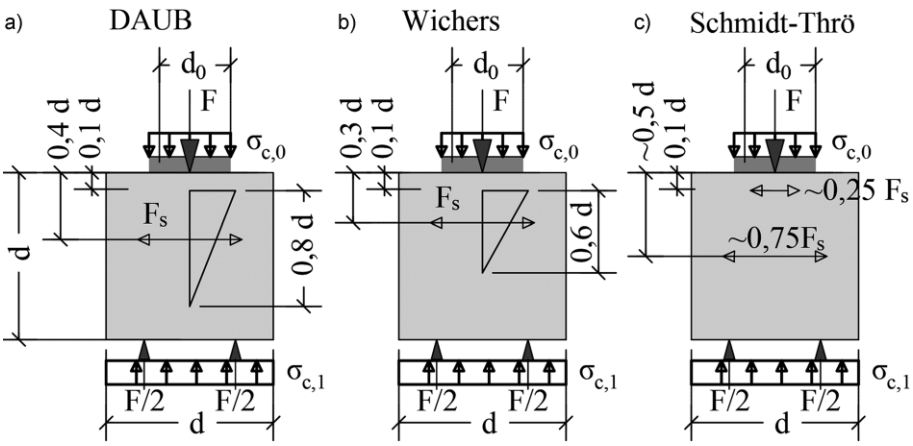

Fig. 5 Recommended centre of gravity of the splitting reinforcement according to a) DAUB [3]; b) Wichers [16]; c) Schmidt-Thrö [6]

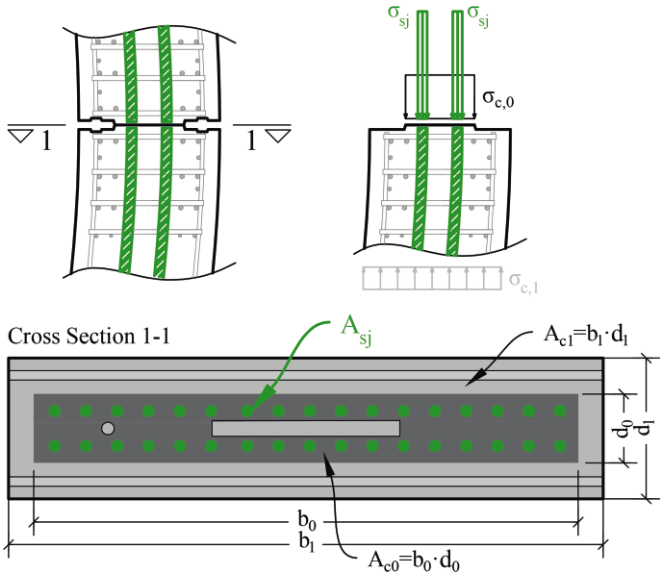

Fig. 6 Newly designed optimized longitudinal joint according to patent application A 50433/2019 [8]

geometrical eccentricities can be done just by adding the load bearing capacity of the longitudinal reinforcement. Following the patent application AT 50433/2019 [8], which was submitted in the beginning of 2019, large-scale tests were performed by the research team of the Institute.

3.1 Experimental investigations

3.1.1 Test specimens

Two different joint reinforcement designs were tested in the course of four experiments. The first test series (Figure 7a) was produced with the conventional reinforcement design (CT = conventional tubbing), the second test series (Figure 7b) with the optimized reinforcement (OT = optimized tubbing) design with the reinforcement bars positioned at the surface of the longitudinal joints. In total there where 16 high strength SAS670/800 reinforcement bars with a diameter of 22 mm placed within the OT-specimens. For the other reinforcement bars in both test series the Austrian standard steel class B550 B was used. The test specimens were 400 mm thick ($d_{1,\mathrm{exp}}$), 700 mm ($b_{1,\mathrm{exp}}$) wide and 600 mm high (exclusive the steel plate). The height of the specimens was chosen by 1.5 times $d_{1,\mathrm{exp}}$ to exclude any load introduction influence on the tubbing joint. For the concrete a strength class of C50/60, with a maximal aggregate size of 16 mm, was chosen. The joint itself was reduced to an area of 605 mm ($b_{0,\mathrm{exp}}$) by 208 mm ($d_{0,\mathrm{exp}}$), resulting in a 55 % smaller cross section than the cross section of the regular tubbing. The geometry of the tubbing was chosen based on a standard tubbing design applied in already existing projects. The chosen thickness correspond to the original size and the width was scaled due to the maximum force application of 18 MN of the testing setup.

Fig. 7 Formwork and reinforcement design of the two test specimen types (figure taken from [20]): a) Conventional tubbing (CT) test specimen; b) Optimized tubbing (OT) test specimen

3.1.2 Test setup

In investigations of tubbing joints conducted in the past by different testing laboratories various approaches for the test setups were adopted. In a test series of Ruhr-Universität Bochum a steel block was utilized for the centric load introduction (shown in Figure 8a) with a PTFE-layer applied in some tests to reduce the transverse strain constraint [5]. In previous tests at TU Wien a UHPC-block was used to transfer the force from the hydraulic jacks into the test specimen (shown in Figure 8b) [21]. In the new test series two segments of the same type were pressed against each other in order to obtain the most realistic test setup as shown in Figure 8c. This resulted in a test setup where the load transferred from one tubbing through the longitudinal joint into the second without any side effects due to load introduction. A similar setup has been used for eccentrically loaded longitudinal joints at the Technical University of Munich [5].

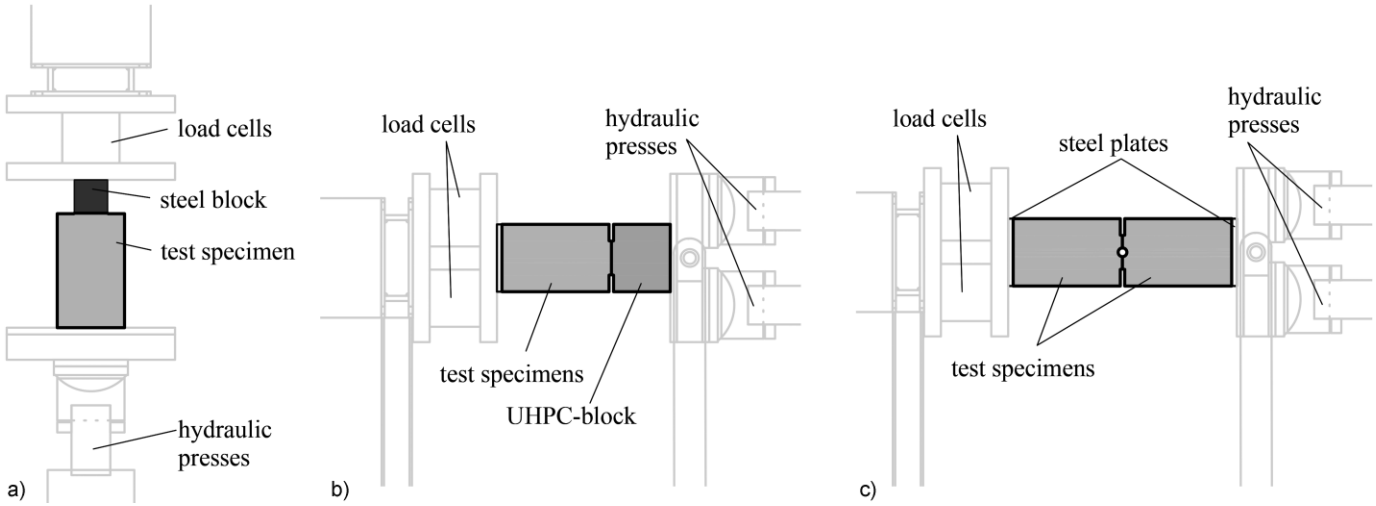

Fig. 8 Test setup approaches: a) Test setup Bochum (2018) [5]; b) Test setup Vienna (2014) [21]; c) Test setup Vienna (2019)

3.1.3 Experimental procedure

After painting the test specimens to improve the visibility of the occurring cracks, the specimens were installed in the test frame. The first test specimen was mounted to the test frame using an adapter steel plate. The second was kept in position with a crane until an axial force of 1000 kN was reached. From that point no additional support was needed. The test segments were installed and tested without any eccentricity. Throughout the experiment, the forces were measured using four load cells and the deformations using four inductive displacement transducers (one per corner). Additionally, the vertical displacements were measured throughout the experiments in four different locations [20]. A photogrammetric measuring system allowed the continuous recording of the crack propagation. The specimens were to be tested in four stages with 15 min hold phases at 30 and 40 % of the calculated ultimate load. In the hold phases the load was kept constant and the existing cracks recorded manually. At 50 % of the ultimate load the load was held for 30 min. At 80 % of the ultimate load the experiment was held again for an hour in order to allow the concrete to creep. This test phase enabled the transfer of the force into the high strength reinforcing steel in the OT-specimens. From that point on the experiment was no longer controlled load-dependent but path-controlled with a speed of < 0.1 mm/min until failure. The total test duration amounted to four to six hours. On a real tunnel construction site, the loads caused by soil and water pressure increase much slower, with the maximum load being reached after a day to a month. The fast load increase leads to a higher ultimate limit load and guarantees conservative test results.

Due to the load transfer in the creep phase, the SAS670/800 in the test OT-specimens were able to be loaded up to their yielding point therefore allowing an economical application. To determine the compressive strain (ε) the mean values of the measured deformations (Δl) were divided by the total length (l_0) of the two test specimens. The force-mean strain diagram of all four experiments is shown in Figure 9. It can be seen that the

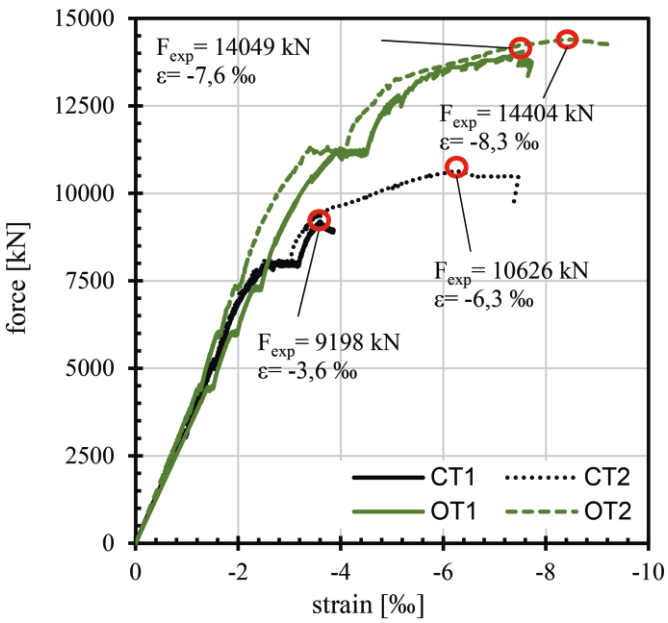

Fig. 9 Force-strain diagram of the four experiments

ductile behaviour of the compressive reinforcement leads to a significant higher failure strain in comparison to the conventionally designed longitudinal joints.

According to the German design guideline for tunnel segments [3] the maximum crack width for the service limit state (SLS) is limited to 0.2 mm. A photogrammetric measuring system allowed the continuous recording of the crack propagation. For the interpretation of the photogrammetric measurements and the concluded positive effect on the SLS for the newly designed longitudinal joint it is referred to Wolfger et al. [20],

4 Discussion of the experimental and calculated results

Up to this point a significant amount of research has been done concerning to the problem of partially loaded areas

Tab. 1 Geometric parameters of the tubbing specimens

$d_{1,exp}$ [mm]	$d_{0,exp}$ [mm]	$b_{1,exp}$ [mm]	$b_{0,exp}$ [mm]	A_{Sl} [mm²]
400	208	700	605	1540

regarding the specific parameters of tubbing joints. Looking at a typical tubbing geometry which was also used in the test series, the calculated load-bearing capacity of a centric loaded longitudinal joint, can be determined with the discussed Eqn. 1, 3 or 6 and the parameters of the experiments summarized in Tab. 1 and Tab. 2. The calculated load-bearing capacity of the joint calculated with Eqn. 1, 3 or 6 lies between 60 and 65 % of the theoretical load-bearing capacity due to normal forces of the regular cross section ($F_{cal,cs}$) according to Eq. 7.

$$F_{cal,cs} = f_{cm} \cdot (A_{c1} - A_{sl}) + f_y \cdot A_{sl} \tag{7}$$

with

A_{sl} Cross section of longitudinal bending reinforcement
f_y Yield strength of longitudinal bending reinforcement

That means for tubbing rings dominated by compressive normal forces the longitudinal joint is always the weakest part of the construction which is decisive for the thickness of the tubbing. In practice bending moments caused by external loads and eccentricities always occur and have to be considered in the tunnel segment design. The eccentric load situation leads to a reduced and eccentrically loaded surface [3, 13]. Basically the location of the longitudinal joint reinforcement can be adapted for every specific load situation and also increases the load bearing capacity of eccentrically loaded longitudinal joints.

In total four specimens were tested. Two tests with a conventional joint design (CT1 and CT2) and two with the optimized longitudinal joint (OT1 and OT2). The test results and all calculations are summarized in Tab. 2. For the calculated failure loads of the test CT-specimens the Eqn. 1, 3, 6 were used and the f_{cd} was replaced by the determined f_{cm} (mean value of concrete cylinder compressive strength seen in Tab. 2). The calculated failure load for the OT-specimens was determined by adding the load-bearing capacity of the additional joint reinforcement ($A_{sj} \cdot f_{sj}$) to the Eqn. 1, 3 or 6. As shown in Eq. 8 any mechanical model can be supplemented with the load-bearing capacity of the additional joint reinforcement. For the presented experiments f_{sj} was taken equal to $f_{ym,SAS670}$.

$$F_{cal.OT} = F_{cal.CT} \cdot \left(\frac{A_{c0} - A_{sj}}{A_{c0}} \right) + A_{sj} \cdot f_{sj} \tag{8}$$

with

$F_{cal.CT}$ Calculated failure load determined by Eqn. 1, 3 or 6
A_{sj} Area of the longitudinal joint reinforcement
f_{sj} Yield strength of the longitudinal joint reinforcement

As can be seen in Tab. 2 for the centric loaded tubbing joint which leads to a A_{c1}/A_{c0}-ratio of about 2.23 all the discussed models lead to a quite similar result. For a reinforcement ratio of 1 % the increase factors (σ_{c0}/f_{cm}) for the concrete strength in dependence of the A_{c1}/A_{c0} ratio of the three presented mechanical models are shown in Figure 10. Especially for higher A_{c1}/A_{c0} ratios the models diverge.

The mean value of the experimental load-bearing capacity of the OT-specimens surpassed that of the CT-specimens by 43 %. This result fits very good to the calculated increasement of 42 to 44 % according to Eq. 8. Based on the variation coefficient of about 10 % of the CT-test series it is highly recommended to proof these results with further experiments.

When it comes to building site conditions and the manufacturing tolerances it is necessary to consider inaccura-

Tab. 2 Material properties, experimental and calculated failure loads of the four test specimens

		CT1	CT2	OT1	OT2
f_{cm}	[N/mm²]	51.9	51.9	51.9	51.9
f_y	[N/mm²]	550	550	550	550
$f_{ym,SAS670}$	[N/mm²]	–	–	776	776
F_{exp}	[kN]	9,198	10,626	14,049	14,404
$F_{exp,mean}$	[kN]	9,912	14,226		
$F_{cal,EC2}$	[kN]	9,742	9,742	13,993	13,993
$F_{cal,Schmidt\text{-}Thrö}$	[kN]	9,919	9,919	14,162	14,162
$F_{cal,Wichers}$	[kN]	9,378	9,378	13,768	13,768
$F_{exp}/F_{cal.EC2}$	[–]	0.94	1.09	1.00	1.03
$F_{exp}/F_{cal.Schmidt\text{-}Thrö}$	[–]	0.93	1.07	0.99	1.02
$F_{exp}/F_{cal.Wichers}$	[–]	0.97	1.12	1.02	1.05

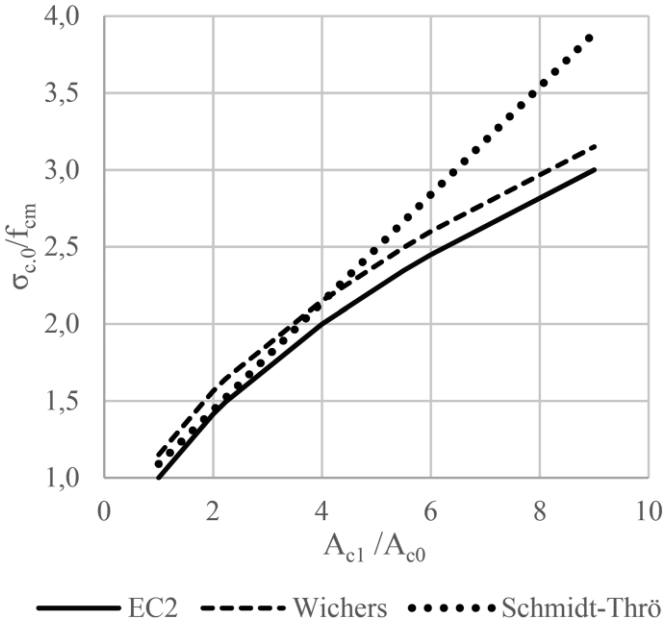

Fig. 10 Load-bearing capacity increase factor σ_{c0}/f_{cm} in dependence of the geometrical ratio A_{c1}/A_{c0}

cies of the position of the additional reinforcement bars. The visualization of the overlap of the butt joint surfaces of the reinforcement bars, depicted in Figure 11, shows that already under laboratory conditions not all bars were positioned on top of each other.

The impact of tubbing segment eccentricities and inaccuracies on the load-bearing capacity and the stiffness of the longitudinal joint of the newly designed tubbing is important when it comes to the application for a tunnel project in practice. Upon this point it is assumed that the confining of the transversal reinforcement has a very positive effect to the load transfer from one continuous reinforcement bar through the butt joint into the second.

5 Conclusion and outlook

The large-scale tests showed that a higher load-bearing capacity of the longitudinal joints was achievable with the newly developed joint design, showing great potential for the construction of tunnels with thinner tubbings and without disadvantages due to corrosion problems in the near future. The following conclusions can be drawn from the investigations presented in this paper:

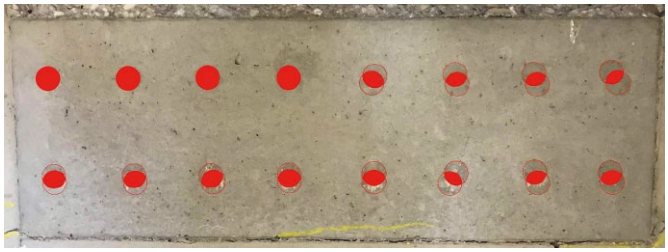

Fig. 11 Overlap of the butt joint surfaces in the longitudinal joint of the tubbings

- Mechanical models: The deviation of the different models when it comes to a higher geometrical ratio of A_{c1}/A_{c0} shown in Figure 10 shows that there is still a lot of potential to improve the existing mechanical models for this specific problem. A design approach which considers the geometrical parameters und the confining effect of the transversal reinforcement is desirable. However, with the suggestion of adding the load-bearing capacity of the additional joint reinforcement every existing and future design approach can be adapted according to current valid guidelines.
- Load bearing-capacity increasement: The experimental increasement of the load-bearing capacity of the optimized tubbing reinforcement confirms the calculated increasement. When it comes to building-site conditions further investigations into the influence of tubbing segment eccentricities with a variable geometrical reinforcement ratio on the load-bearing capacity and stiffness of the longitudinal joint have to be done.

Especially the behaviour of the load transfer from one continuous reinforcement bar through the butt joint into the second has to be investigated to be able to optimize the reinforcement of a tunnel segment for every single tunnel project and there specific requirements due to load and eccentricities.

Acknowledgement

The experiments were supported by Stahlwerk Annahütte Max Aicher GmbH & Co. KG which provided the SAS670/800 reinforcement bars.

References

[1] ÖNORM EN 1992-1-1 (2015) *Design of concrete structures: Part 1-1: General rules and rules for buildings*. Vienna: Austrian Standards Institute.

[2] ÖNORM B 1992-1-1 (2018) *Design of concrete structures: Part 1-1: General rules and rules for buildings*. Vienna: Austrian Standards Institute.

[3] DAUB (2013) *Empfehlungen für den Entwurf, die Herstellung und den Einbau von Tübbingringen*. Köln: Deutscher Ausschuss für unterirdisches Bauen.

[4] ÖVBB (2009) *Tübbingsysteme aus Beton*. Wien: Österreichische Vereinigung für Beton- und Bautechnik.

[5] Schmidt-Thrö, G., Smarslik, M., Tabka, B., et al. (2019) *Experimental analysis of concrete elements under partial area strip loading* in: Civil Engineering Design 1(1), 28–38. https://doi.org/10.1002/cend.201900001

[6] Schmidt-Thrö, G. (2019) *Zum Tragverhalten der Tübbinglängsfuge*. [Dissertation]. Technische Universität München, http://mediatum.ub.tum.de/doc/1484068/document.pdf.

[7] Kollegger, J., Proksch-Weilguni, C., Wolfger, H. (2020) *Reinforced concrete tubbing*. PCT patent application PCT/AT2020/060030, submitted 4th February 2020.

[8] Kollegger, J., Proksch-Weilguni, C., Wolfger, H. (2019) *Tübbing aus bewehrtem Beton*. AT patent application A 50433/2019, submitted 14th May 2019.

[9] Porr Bau GmbH (2016) *Verbundsegment, Tunnelschale und Verfahren*. AT patent application AT 518840 A1, publicated 24th June 2016.

[10] Dahl, J. (2002) *Tubing segment for a tunnel lining, in particular a high performance tubing element*. EP patent EP 1 243752 B1, granted 23rd Mai 2007.

[11] Oger, J.F.M. (1977) *Ausbauelement für den Schachtausbau oder dergleichen und Verfahren zu seiner Herstellung*. DE patent DE 25 22 789 C3, granted 8th December 1977.

[12] Hirohide, H., Susumu, U. (1999) *Joint structure of segment*. JP patent application 11287093, submitted 19th October 1999.

[13] Fischer, O., Schmidt-Thrö, G. (2016) *Bemessung und Konstruktion von Längsfugen beim Tübbingausbau* in: DGGT [Hrsg.] Taschenbuch für den Tunnelbau, pp. 81–134. Berlin: Ernst & Sohn

[14] Mörsch, E. (1924) *Über die Berechnung der Gelenkquader* in: Beton Eisen 23 Heft Nr. 12, S. 156–161

[15] Grasser, E., Thielen, G. (1972) *Hilfsmittel zur Berechnung der Schnittgrößen und Formänderungen von Stahlbeton* (DAfStb Heft 240). Berlin: Ernst & Sohn

[16] Wichers, M. (2013) *Bemessung von bewehrten Betonbauteilen bei Teilflächenbelastung unter Berücksichtigung der Rissbildung*. Institut für Baustoffe, Massivbau und Brandschutz IBMB, https://nbn-resolving.org/urn:nbn:de:gbv:084-13052911495.

[17] Wurm, P., Daschner, F. (1983) *Teilflächenbelastung von Normalbeton Versuche an bewehrten Scheiben* (DAfStb Heft 344). Berlin: Ernst & Sohn

[18] Bauschinger, J. (1876) *Versuche mit Quadern aus Naturstein* in: Mitteilungen aus dem Mechanisch Technischen Laboratorien der Technischen Hochschule München 6, 1–20

[19] Spieth, H.P. (1959) *Das Verhalten von Beton unter hoher örtlicher Pressung und Teilbelastung unter besonderer Berücksichtigung von Spannbetonverankerungen*. [Dissertation]. Technische Hochschule Stuttgart.

[20] Wolfger, H., Proksch-Weilguni, C., Kollegger, J. (2021) *Longitudinal joints of tubbings with newly designed high-strength reinforcement* in: Structural Concrete. https://doi.org/10.1002/suco.202000670

[21] Träger, W. (2014) *Versuche zur Ermittlung der Tragfähigkeit der Tübbing-Längsfuge*. Wien: TU Wien.

Authors

Dipl.-Ing. Clemens Proksch-Weilguni
(corresponding author)
clemens.proksch-weilguni@tuwien.ac.at
Technische Universität Wien
Institute of Structural Engineering – Research Unit
Structural Concrete
Karlsplatz 13
1040 Vienna
Austria

Dipl.-Ing. Hannes Wolfger
hannes.wolfger@tuwien.ac.at
Technische Universität Wien
Institute of Structural Engineering – Research Unit
Structural Concrete
Karlsplatz 13
1040 Vienna
Austria

Univ.Prof. Dipl.-Ing. Dr.techn. Johann Kollegger
johann.kollegger@tuwien.ac.at
Technische Universität Wien
Institute of Structural Engineering – Research Unit
Structural Concrete
Karlsplatz 13
1040 Vienna
Austria

How to Cite this Paper

Proksch-Weilguni, C.; Wolfger, H.; Kollegger, J. (2021) *Optimized reinforcement in longitudinal joints of segmental tunnel linings*. Geomechanics and Tunnelling 14, No. 4, pp. 390–399.
https://doi.org/10.1002/geot.202000046

This paper has been peer reviewed. Submitted: 6. November 2020; accepted: 16. March 2021.